This paper is published as part of a *Dalton Transactions* themed issue on:

Metal Anticancer Compounds

Guest Editor Peter Sadler

University of Warwick, UK

Published in issue 48, 2009 of *Dalton Transactions*

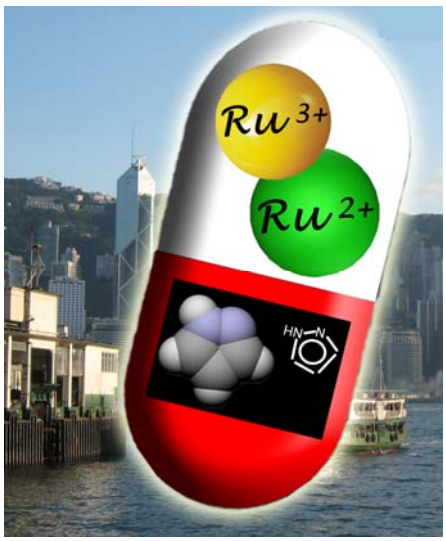

Image reproduced with permission of Chi-Ming Che

Articles published in this issue include:

PERSPECTIVES:

Non-traditional platinum compounds for improved accumulation, oral bioavailability, and tumor targeting
Katherine S. Lovejoy and Stephen J. Lippard, *Dalton Trans.,* 2009, DOI**:** 10.1039/b913896j

Metal complexes as photochemical nitric oxide precursors: Potential applications in the treatment of tumors
Alexis D. Ostrowski and Peter C. Ford, *Dalton Trans.,* 2009, DOI: 10.1039/b912898k

Novel and emerging approaches for the delivery of metallo-drugs
Carlos Sanchez-Cano and Michael J. Hannon, *Dalton Trans.,* 2009, DOI: 10.1039/b912708a

HOT ARTICLE:

Iron(III) complexes of fluorescent hydroxamate ligands: preparation, properties, and cellular processing
Antonia J. Clarke, Natsuho Yamamoto, Paul Jensen and Trevor W. Hambley**,** *Dalton Trans.,* 2009, DOI**:** 10.1039/b914368h

Visit the *Dalton Transactions* website for more cutting-edge inorganic and bioinorganic research
www.rsc.org/dalton

The role of bridging ligands in determining DNA-binding ability and cross-linking patterns of dinuclear platinum(II) antitumour complexes†

Jianhui Zhu,[a] Miaoxin Lin,[a] Damin Fan,[a] Ziyi Wu,[a] Yuncong Chen,[a] Junfeng Zhang,[b] Yi Lu[c] and Zijian Guo*[a]

Received 3rd July 2009, Accepted 28th October 2009
First published as an Advance Article on the web 13th November 2009
DOI: 10.1039/b913236h

The DNA binding ability and binding mode of platinum complexes are crucial factors that govern their cytotoxic activity. In this work, circular dichroism spectroscopy, gel electrophoresis and MALDI-TOF MS spectrometry combined with enzymatic degradation have been used to elucidate the role of bridging ligands in DNA-binding ability and cross-linking patterns of two dinuclear antitumour active platinum(II) complexes, {[*cis*-Pt(NH_3)$_2$Cl]$_2$L1}(NO_3)$_2$ (**1**, L1= 4,4′-methylenedianiline) and {[*cis*-Pt(NH_3)$_2$Cl]$_2$L2}(NO_3)$_2$ (**2**, L2 = α,α′-diamino-*p*-xylene). Although both complexes have two *cis*-diammine-Pt(II) moieties (1,1/c,c), complex **1** exhibits much higher DNA-binding ability than complex **2**. The former readily forms both 1,3- and 1,4-intrastrand cross-links with DNA oligonucleotides, while the latter preferentially forms 1,4- rather than 1,3-intrastrand cross-links. Cytotoxicity studies against a human non-small-cell lung cancer cell line (A549) demonstrate that complex **1** has higher activity than **2**. These results show that the linker properties play a critical role in controlling the DNA-binding and cross-linking abilities and in modulating the cytotoxicity of dinuclear platinum complexes.

Introduction

Polynuclear platinum complexes represent a novel class of platinum-based agents that have shown great potential for cancer thermotherapy.[1-3] These compounds distinguish themselves from cisplatin and its mononuclear analogues by forming DNA long-range intra- and interstrand cross-links.[4-6] This unique DNA binding feature is believed to be responsible for their distinctive cytotoxicity profile.[6-8] It also affords great potential to overcome the recognition and elimination of cisplatin-GG cross-links by proteins evolved in the nucleotide excision-repair (NER) pathway.[9-10]

Farrell and co-workers have designed a series of polynuclear platinum(II) complexes with both *cis*- and/or *trans* configurations bridged by linear aliphatic diamines that demonstrate great clinical potential.[11-14] The linker properties such as length, flexibility, hydrogen-bonding capacity are major factors that facilitate long-range cross-links and govern the antitumour activity.[15-18] One of the most outstanding examples of these complexes is BBR3464 (1,0,1/t,t,t), which contains two active mono-functional Pt centers and a third coordinatively saturated Pt(II) centre. This compound exhibits great antitumour activities against pancreatic, lung and melanoma cancers and is in phase II clinical studies.[19,20] These studies led to an effective and promising strategy in designing novel Pt(II)-based anticancer drugs, although some difficulties such as glutathione (GSH) induced drug degradation need to be overcome.[21]

[a]*State Key Laboratory of Coordination Chemistry, School of Chemistry and Chemical Engineering, Nanjing University, Nanjing, 210093, China. E-mail: zguo@nju.edu.cn; Fax: +86-25-83314502*
[b]*State Key Laboratory of Pharmaceutical Biotechnology, Nanjing University, Nanjing, 210093, China*
[c]*Department of Chemistry, University of Illinois at Urbana-Champaign, Urbana, Illinois, 61801, USA*

† Electronic supplementary information (ESI) available: Experimental details and characterization data. See DOI: 10.1039/b913236h

Recently we reported a 1,1/c,c dinuclear platinum(II) complex containing an aromatic linker, {[*cis*-Pt(NH_3)$_2$Cl]$_2$L1}(NO_3)$_2$ (**1**, L1= 4,4′-methylenedianiline, Scheme 1).[22] This compound demonstrates higher cytotoxicity against P388 and A549 cell lines than cisplatin. It is interesting to note that due to the presence of phenyl groups in the linker complex **1** showed high inertness towards GSH, a favorable property that may help to reduce GSH-associated side effects and thereby increase therapeutic efficacy.[23]

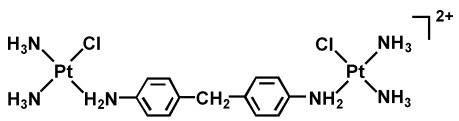

1

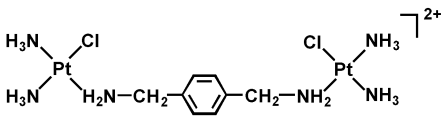

2

Scheme 1 Structures of complexes **1** and **2**.

Herein, we describe a comparison of **1** and its analogue, a 1,1/c,c dinuclear platinum complex {[*cis*-Pt(NH_3)$_2$Cl]$_2$L2}(NO_3)$_2$ (**2**, L2 = α,α′-diamino-*p*-xylene, Scheme 1) to further understand the role of the linker in modulating their DNA-binding and antitumour properties. Two DNA oligonucleotides **N1** 5′-d(CTTGTTGTCACATGAT)-3′·5′-d(ATCATGTGACAACAAG)-3′ and **N2** 5′-d(GAAGAAGTCACAAAATGT)-3′·5′-d(ACATTTTGTGACTTCTTC)-3′ (Scheme 2) are used, which offer three potential reactive sites of 1,3- and 1,4-intrastrand (GG) and 1,3-interstrand (GG).

N1: 5′-CTT**G**TT**G**TCACATGAT-3′ (OD1)
3′-GAACAACA**G**T**G**TACTA-5′ (OD2)

N2: 5′-GAA**G**AA**G**TCACAAAATGT-3′
3′-CTTCTTCA**G**T**G**TTTTACA-5′

N3: 5′-GAA**G**AA**G**TCACAAAATGT-3′
3′-TCAACTTCTTCA**G**T**G**TTTTACA-5′

Scheme 2 Oligonucleotide duplexes **N1**, **N2** and **N3** employed in this work.

Experimental

Materials

Complexes **1** and **2** were prepared as described in previous work[22] or in the ESI.†

Single-stranded oligonucleotides OD1 and OD2, 5′-FAM-labeled DNA duplex **N2**, 5′-FAM blunt-end-labeled duplex **N3**, and pUC 19 plasmid DNA were purchased from TaKaRa (Bio Inc., Tokyo). All oligonucleotides used in this study were purified by HPLC. The single strands OD1 and OD2 were respectively 5′-labeled with [γ-^{32}P]-ATP (from Perkin-Elmer) using T4 kinase purchased from Invitrogen, purified by a Sep-Pak C18 column (Waters Corp., Milford, MA), then annealed with the unlabeled complementary strand in a 95 °C water bath for 2 min, and subsequently cooled slowly to room temperature to form duplex **N1** with a 5′-^{32}P-label on one strand. Calf thymus DNA (CT-DNA) and tris(hydroxymethyl)aminomethane (Tris) were from Sigma. Exonuclease III was purchased from Promega (Madison, WI). 3-Hydroxypicolinic acid (HPA) was purchased from Bruker Daltonics (Billerica, MA).

Instrumentation and methods

The circular dichroism (CD) spectra were explored on a Jasco J-810 spectropolarimeter in a 1 cm path length cylindrical quartz cell. Each sample solution in Tris-HCl buffer (pH = 7.4, 50 mM Tris-HCl, 50 mM NaCl) was incubated for 12 h at room temperature before measurement and scanned from 320 to 220 nm at a speed of 10 nm min^{-1}. The concentration of CT-DNA was 1.033×10^{-4} M.

Mass spectra were recorded on a Bruker Autoflex II MALDI-TOF MS (Bruker Daltonics) equipped with a 337 nm N_2 laser set to a repetition rate of 25 Hz and performed in a linear negative ion mode. The mass range was *m/z* 500–14 000. DNA samples were desalted using a ZipTip® pipette tip C18 (Millipore Corp., Bedford, MA). The MALDI matrix solution (0.5 μL), containing 3-hydroxypicolinic acid, diammonium citrate and acetonitrile, was deposited onto the sample target disk and air-dried. The purified DNA products (0.5 μL) were placed on the top of the crystallized matrix spot and allowed to air-dry *prior to* analysis.

DNA unwinding was examined by electrophoretic mobility shift assays through 1% agarose gel with TAE buffer (40 mM Tris acetate, 1 mM EDTA), using pUC 19 plasmid DNA (200 ng) incubated with complex **2** at 37 °C for 24 h with input drug-to-nucleotide ratios (r_i) from 0.015 to 0.24. The resultant gel was stained with 0.5 μg mL^{-1} ethidium bromide in TAE buffer and visualized under UV light.

The platination of duplexes **N1** or **N2** by complexes **1** and **2** was studied by using 20% polyacrylamide denaturing gels (7 M urea). The duplexes at a concentration of 2 μM were incubated with complexes at 37 °C at platinum-to-strand molar ratios of 1 or 2. The reaction was quenched by adding 5 μL of formamide loading buffer, heated at 90 °C for 2 min and then cooled on ice. After gel separation, DNA bands were cut out respectively, crushed, and soaked in a solution of 10 mM Tris buffer and 1 mM EDTA (pH 7.6). Then the samples were pooled and desalted using Sep-Pak C18 columns (Waters Corp., Milford, MA), lyophilized, and dissolved in deionised water for subsequent MALDI-TOF MS detection.

Exonuclease III Digestion of DNA adducts was explored by incubating platinated duplex **N3** (20 pmol, Scheme 2) with 4 U of exonuclease III in 1× Exo III reaction buffer (66 mM Tris-HCl, pH 8.0, 0.66 mM $MgCl_2$) at 37 °C for 10 min (total volume = 20 μL) and quenched by adding EDTA to a final concentration of 25 mM. Samples were analyzed by MALDI-TOF MS following the desalting procedure described above.

The growth inhibitory effect of complex **1**, **2** and cisplatin against the human non-small-cell lung cancer cell line A-549 was measured by the sulforhodamine B (SRB) assay.[24]

Results and discussion

Circular dichroism spectroscopy

The DNA binding ability of complex **2** was studied by circular dichroism spectra and compared with that of **1**. The spectrum of CT-DNA alone exhibited a positive band at 275 nm due to base stacking and a negative band at 245 nm due to the helicity of B-type DNA.[25] As shown in Fig. 1, the addition of complex **2** induced an apparent decrease in ellipticity and a gradual red shift for both negative and positive bands (spectra b–f), which suggested the unwinding of the DNA helix and a tendency of conformation deviation from B-DNA to Z-DNA. However, comparison with the data of complex **1**[22] revealed that the conformation changes induced by **2** were less remarkable.

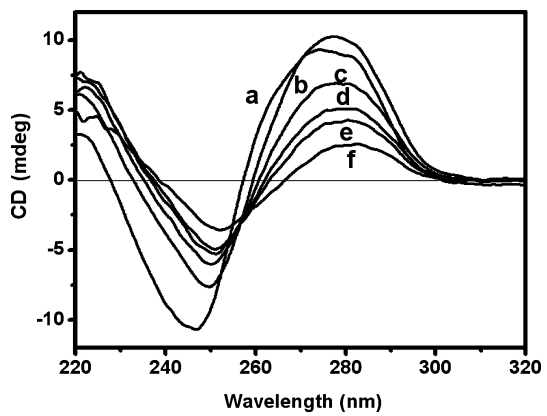

Fig. 1 Circular dichroism (CD) spectra of calf thymus DNA (1×10^{-4} M) under different concentration ratios of complex **2** to DNA: (a) 0, (b) 0.1, (c) 0.2, (d) 0.4, (e) 0.6 and (f) 0.8, respectively.

DNA unwinding

DNA unwinding properties of complexes **1** and **2** were further explored by native agarose gel electrophoresis using pUC 19 plasmid DNA. As shown in Fig. 2, an obvious decrease in the

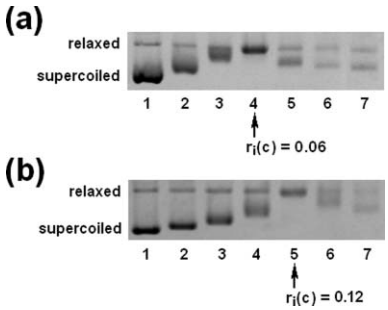

Fig. 2 Electrophoresis in agarose gels of pUC19 plasmid DNA incubated with complexes **1** (a) and **2** (b) at 37 °C for 24 h. Lane 1, DNA control, lanes 2–7, r_i values of 0.015, 0.03, 0.06, 0.12, 0.18, 0.24, respectively.

mobility of supercoiled DNA was observed upon incubation with **1** and **2**, indicating the unwinding of DNA duplex.[26] In contrast, the mobility of relaxed DNA was slightly accelerated, suggesting the condensation of DNA helix due to DNA diadducts formed by platinum complexes.[27] With the increase of the input molar ratio of complex to nucleotide (r_i), the separation between supercoiled and relaxed DNA was conspicuously decreased. The coalescence point $r_i(c)$, corresponding to the full relaxation of the supercoiled DNA which co-migrated with relaxed DNA, was 0.06 for complex **1** (Fig. 2a) and 0.12 for complex **2** (Fig. 2b). Under the same experimental conditions, cisplatin displayed a slower tendency for the two DNA forms and a coalescence point was not observed even at $r_i = 0.36$ (data not shown). The result suggests that complex **1** exerts more perturbation on the tertiary structure of supercoiled DNA than **2** and cisplatin, which is consistent with the CD results.

Cytotoxicity assays

The cytotoxicity of complex **2** was evaluated against the human non-small-cell lung cancer cell line (A549) and compared with that of complex **1**, with cisplatin as a positive control (Fig. 3). At all concentrations (10^{-4}–10^{-6} M), both complexes **1** and **2** demonstrated much higher cytotoxic potency than cisplatin. Complex **1** exhibited more significant antitumour activity than **2**. In particular, at the concentration of 10^{-6} M, complex **1** maintained a high inhibition rate of 57.4%,[22] while the inhibition rate induced by **2** and cisplatin was only 27.7% and 6.2%, respectively.

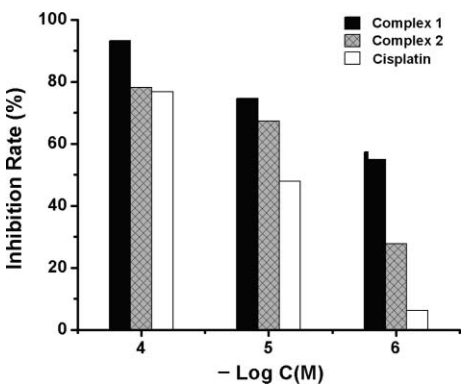

Fig. 3 Cytotoxic activity of complexes **1**, **2** and cisplatin against the human nonsmall-cell lung cancer cell line (A549).

From the results of the above mentioned experiments, complex **1** showed superior DNA binding ability, a higher antitumour activity than complex **2**. It is therefore indispensable to investigate their DNA adducts in further detail and to correlate with the structural differences of the linker.

Platination of oligonucleotides

To investigate the difference in DNA cross-linking patterns, the duplex **N1**, OD1[5′-d(CTT**G**TT**G**TCACATGAT)-3′]·OD2[5′-d(ATCAT**GTG**ACAACAAG)-3′], with 5′-^{32}P-labels on strand OD1 or OD2 which corresponded to the potential reactive sites for 1,4- and 1,3-GG cross-links respectively, was incubated with complex **1** or **2** for 12 h at as platinum-to-strand molar ratio of 1 : 1 at 37 °C, then loaded on to a 20% polyacrylamide denaturing gel.

As shown in Fig. 4, two sets of DNA bands occurred after incubation with complex **1** or **2**, representing platinum-modified DNA lesions. According to their electrophoretic mobilities, these bands were assigned to the following adducts: mono-adducts of **1** (marked as $\mathbf{a_1}$) and **2** (marked as $\mathbf{a_2}$), and intrastrand cross-links of **1** (marked as $\mathbf{b_1}$) and **2** (marked as $\mathbf{b_2}$). Interstrand cross-links were not observed under these experimental conditions. Two DNA bands were observed in the region of $\mathbf{b_1}$ in lane 2, with the dark-band as the major DNA adduct, which can be assigned to the 1,3-GG intrastrand cross-link. The light-band may correspond to different intrastrand cross-linking modes although it could not be assigned unambiguously. The DNA bands in the region of $\mathbf{a_2}$ in lanes 3 and 4 can be attributed to the formation of monoadducts and di-monoadducts in which one or two platinum compounds were bound to different DNA bases, respectively.

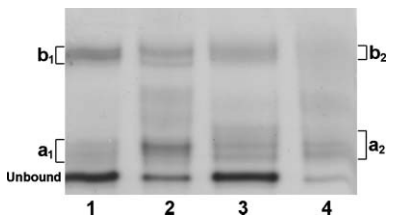

Fig. 4 Autogradiogram of a 20% polyacrylamide denaturing gel (7 M urea) showing DNA adducts of duplex **N1**, with 5′-^{32}P-labeled *OD1 or *OD2, respectively. Lane 1: *OD1-labeled **N1** with complex **1**, lane 2: *OD2-labeled **N1** with complex **1**, lane 3: *OD1-labeled **N1** with complex **2**, lane 4: *OD2-labeled **N1** with complex **2**.

Interestingly, complex **1** can readily form intrastrand cross-links both on the strand *OD1 (lane 1) and on the strand *OD2 (lane 2), corresponding to 1,4- and 1,3-intrastrand cross-links respectively. However, in the case of complex **2**, only intrastrand cross-links on the strand *OD1 (lane 3) were observed, suggesting a preference for the 1,4-intrastrand cross-link. The result reveals that equivalent amounts of 1,4- and 1,3-intrastrand cross-links can be readily formed by complex **1**, whereas the 1,3-intrastrand cross-link is less favorable for complex **2**, which should be relevant to the more flexible linker in complex **1** than that of **2**. Geometry optimization of complexes **1** and **2** calculated at the HF/6-31G** level using the Gaussian 03 program[28] illustrates that the Pt···Pt distances are 13.12 Å in **1** and 11.31 Å in **2** respectively (Fig. S2†). The sp^3-hybridized orbital character of methylene carbon determines that **1** is a nonplanar molecule. The coordination sphere has a significant effect on the dihedral angle between the two phenyl planes, which

leads to a flexible intrametal distance as demonstrated by the X-ray crystal structures of a series of dinuclear iron and ruthenium complexes with the di(4-phenyl)methane linker.[29] It is possible that the Pt···Pt distance can be altered by the spacing of the two phenyl rings, when two Pt centers in **1** coordinate to *N*7 of the guanines, giving the formation of 1,3- and 1,4-intrastrand cross-links. However, the bridging linker of diamino-*p*-xylene in **2** suggests that the two methylenes are in the plane of the phenyl ring, leading to a greater rigidity of complex **2** and the predominant formation of 1,4-intrastrand cross-links.

MALDI-TOF MS spectroscopy

MALDI-FOF MS has been used recently to identify the formation of Pt-DNA adducts.[30-32] After incubation of complexes **1** and **2** with unlabeled duplex **N1**, all DNA bands, including unbound DNA and DNA adducts, were extracted separately from gels and desalted by using C18 Zip-tips *prior to* MALDI-TOF MS analysis. The results of MS spectra are illustrated in Fig. 5 and the detailed assignment of each individual peak is listed in Table 1. No peak at *m/z* values over 6000 is observed, suggesting that neither **1** nor **2** formed 1,3-interstrand cross-linking adducts, which is consistent with the results of gel electrophoresis.

Table 1 MALDI-TOF analysis of DNA adducts of complexes **1** and **2** formed with duplex **N1**

Peaks Calcd	Species	Found $[M-H]^-$	
A	{OD1}	4812.4	4812.2
B	{OD2}	4946.5	4946.3
C	{OD1 + $Pt(NH_3)_2$}	5039.3	5039.4
D	{OD2 + $Pt(NH_3)_2$}	5173.1	5173.5
E	{OD1+ [*cis*-$Pt(NH_3)_2$]L1}	5236.9	5238.2
F	{OD2 + [*cis*-$Pt(NH_3)_2$]L1}	5371.6	5372.5
G	{OD1 + [*cis*-$Pt(NH_3)_2]_2$L1}	5464.7	5465.2
H	{OD2+ [*cis*-$Pt(NH_3)_2]_2$L1}	5599.6	5599.5
I	{OD1 + [*cis*-$Pt(NH_3)_2]_2$L2}	5402.7	5403.4
J	{OD2 + [*cis*-$Pt(NH_3)_2]_2$L2}	5536.0	5537.7
L	{OD1 + [*cis*-$Pt(NH_3)_2$]L2}	5174.9	5175.2

Fig. 5a shows the unplatinated DNA after reaction with **1** and **2**, where peaks **A** (*m/z* 4812.4) and **B** (*m/z* 4946.5) correspond to the intact strands OD1 ($[M-H]^-$) and OD2 ($[M-H]^-$), respectively. Two peaks **G** (*m/z* 5464.7) and **H** (*m/z* 5599.6) are observed in the spectra of adducts $\mathbf{a_1}$ (Fig. 5b), which can be assigned to

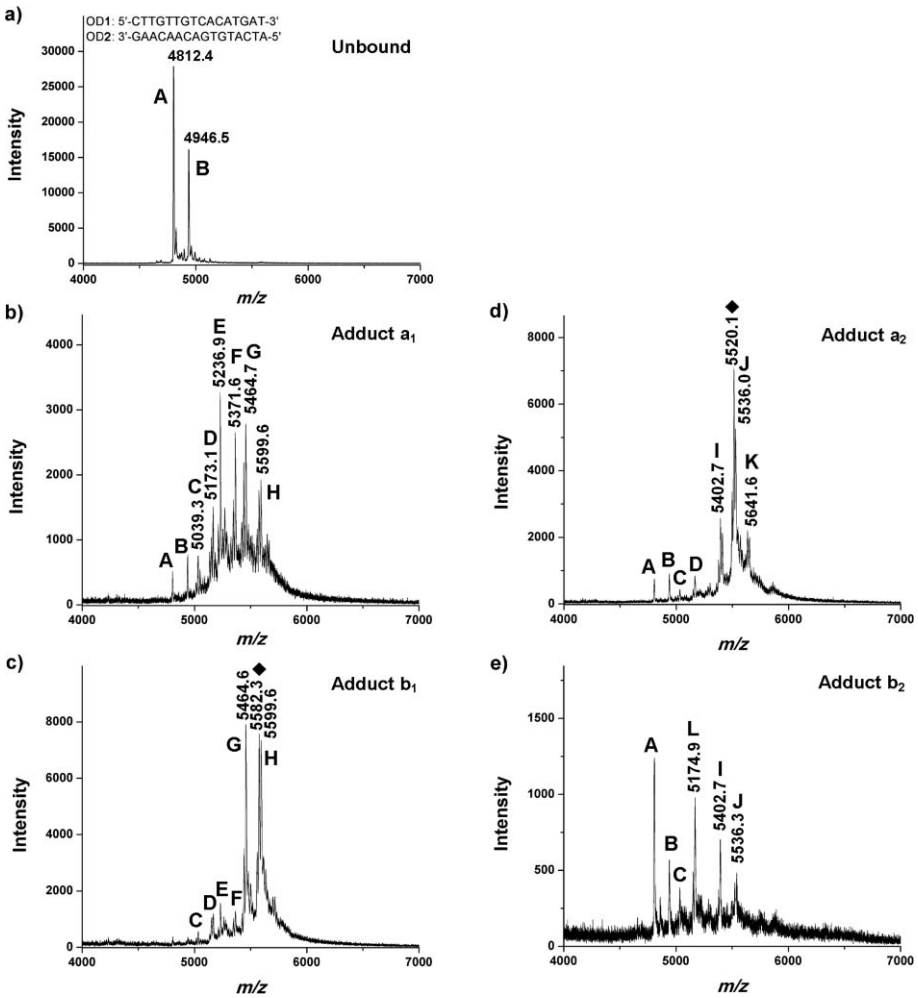

Fig. 5 MALDI-TOF mass spectra of unplatinated **N1** (a), adducts of complexes **1** (b, c) and **2** (d, e) after reaction with **N1** for 12 h. Peaks **A** and **B** represent the unplatinated strand OD1 and OD2, respectively. Peaks **C**, **D**, **E**, **F**, **G**, **H** correspond to adducts of **1**, and **I**, **J**, **L** to those of **2**. Peak **K** corresponds to unidentified species. Adducts with the loss of NH_3 ligand are marked with ◆.

monoadducts with one chloro ligand lost during the MALDI-TOF experiment.[6,33] In the case of $\mathbf{b_1}$ (Fig. 5c), the intensity of peaks **G** and **H** significantly increases, which can be attributed to cross-linked adducts {OD1 + [*cis*-$Pt(NH_3)_2]_2$L1} and {OD2 + [*cis*-$Pt(NH_3)_2]_2$L1}, respectively. The results demonstrate that complex **1** can readily form both 1,3- and 1,4-intrastrand cross-links, which is in good agreement with the result of gel electrophoresis. Several other peaks in Fig. 5b and 5c, such as **C**, **D**, **E** and **F**, can be assigned to {OD1 + $Pt(NH_3)_2$}, {OD2 + $Pt(NH_3)_2$}, {OD1 + [*cis*-$Pt(NH_3)_2$]L1} and {OD2 + [*cis*-$Pt(NH_3)_2$]L1}, respectively. The only possible explanation for the appearance of these peaks is the fragmentation of the adducts in the MALDI-TOF process.[6,33] The same situation occurred in the case of adducts $\mathbf{a_2}$ and $\mathbf{b_2}$ (Fig. 5d and 5e). The peak (*m*/*z* 5582.3) marked with ◆, with a *m*/*z* value of **H** −17.3, may correspond to the loss of one NH_3 ligand.

The MALDI-TOF spectra of adducts $\mathbf{a_2}$ and $\mathbf{b_2}$ of complex **2** are shown in Fig. 5d and 5e, respectively. Peaks **I** (*m*/*z* 5402.7) and **J** (*m*/*z* 5536.0) in Fig. 5d can be assigned to the monoadducts, which were observed in the polyacrylamide gel, with one chloro ligand removed during the MALDI-TOF experiment. In the spectra of $\mathbf{b_2}$ (Fig. 5e), peaks **I** and **J** can be identified as 1,4-intrastrand cross-links {OD1 + [*cis*-$Pt(NH_3)_2]_2$L2} and 1,3-intrastrand cross-links {OD2 + [*cis*-$Pt(NH_3)_2]_2$L2}, respectively. The two intense fragment peaks **A** and **L** (*m*/*z* 5174.9), which can only be derived from the adduct {OD1 + [*cis*-$Pt(NH_3)_2]_2$L2}, suggest that the total amount of 1,4-intrastrand cross-links is much higher than 1,3-cross-links, confirming that complex **2** predominantly forms 1,4-intrastrand cross-links.

Sequence independence of cross-links

We also explored the adducts of complexes **1** and **2** induced in duplex **N2** 5′-d(GAA**G**AA**G**TCACAAAATGT)-3′·5′-d(ACATTTT**GTG**ACTTCTTC)-3′, which was originated from breast/ovarian cancer susceptibility genes BRCA1 (Genbank #U14680).[34] Except for the different bases flanking the active guanines (G), duplex **N2** has the same potential reactive sites as duplex **N1**, which are 1,3-GG and 1,4-GG intrastrand cross-links, and 1,3-GG interstrand cross-links.

As shown in Fig. S3,† a similar result was obtained for duplex **N2**. Mono-adducts $\mathbf{a_1}$ and $\mathbf{a_2}$ and intrastrand cross-links $\mathbf{b_1}$ and $\mathbf{b_2}$ were the major adducts formed by complexes **1** and **2**, respectively. Two DNA bands with the equivalent intensity in the region of $\mathbf{b_1}$ can be ascribed to 1,3- and 1,4-intrastrand cross-links of complex **1** based on their different migration abilities in gels. In contrast, only one clear DNA band was observed at the platinum-to-strand ratio of 1 : 1 in the region of $\mathbf{b_2}$, which can be assigned to 1,4-intrastrand cross-links. A minor band which is assignable to 1,3-intrastrand cross-links occurred only in the presence of excess complex **2**. The results demonstrate again that complex **1** can readily form 1,3- and 1,4-intrastrand cross-links and complex **2** predominantly gives rise to 1,4- intrastrand cross-links.

Kinetic analysis

The time dependence of the formation of DNA cross-links of **1** and **2** with **N2** was measured at 37 °C, by stopping the reaction at an appropriate time of 0.5, 2, 5, 12 and 24 h, followed by a 20% ployacrylamide denaturing gel (Fig. 6a). The percentage of each

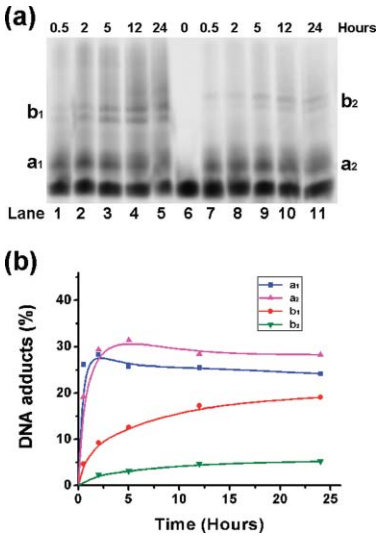

Fig. 6 Kinetics for the formation of adducts in the duplex **N2** by complexes **1** and **2** at the platinum-to-strand ratio of 1. (a) Image of a 20% polyacrylamide denaturing gel. Lanes 1–5: complex **1**, lane 6: DNA control, lanes 7–11: complex **2**. (b) Proportion of DNA adducts calculated from the ratio of the intensity of each adduct band to the intensity sum of all bands. (■:$\mathbf{a_1}$, ▲: $\mathbf{a_2}$, ●: $\mathbf{b_1}$, ▼: $\mathbf{b_2}$).

DNA adduct is shown in Fig. 6b. In the case of **1**, mono-adducts $\mathbf{a_1}$ was rapidly formed, with the maximum intensity attained in less than 2 h, followed by a slight decrease. However, in the case of **2**, mono-adducts $\mathbf{a_2}$ reached its maximum intensity after 5 h incubation. Similarly, the formation of cross-linking adducts $\mathbf{b_1}$ was much faster than that of $\mathbf{b_2}$. The amount of $\mathbf{b_2}$ was accounted for by only 5.2% even after 24 h incubation. The result suggests the DNA cross-linking reaction of complex **1** is more effective than that of **2**. Again, the nature of the linker moiety in **1** and **2** plays a determining role in the kinetic formation of DNA adducts.

Inhibition of exonuclease digestion

The DNA adducts of **1** and **2** were further enzymatically digested and subsequently analyzed by MALDI-TOF MS to determinate the platination sites on DNA. Exonuclease III, which can generate DNA ladders by sequentially removing nucleotides from the 3′-end of duplex DNA,[35] was used in this study. To obtain unidirectional digestion, duplex **N3** (Scheme 2), which is identical to duplex **N2** except for one 3′-overhang on the bottom strand that is resistant to Exo III cleavage,[36] was incubated with complexes for 12 h before enzymatic degradation. Under the same experimental conditions, the unplatinated duplex **N3** was completely digested, resulting in progressive deletions of nucleotide from the blunt-ended strand OD3 (ESI, Fig. S4†).

Fig. 7a shows the digestion of DNA adducts of duplex **N3** of complex **1**. Peak at *m*/*z* 6765.6 corresponds to the intact cross-linking adducts {OD3 + [*cis*-$Pt(NH_3)_2Cl]_2$L1}. Six new peaks, deriving from the digestion fragments of this adduct, were observed, with consecutive removal of the first nine residues, *i.e.* –T (*m*/*z* = 6463.3), –TG (*m*/*z* = 6131.8), –TGT (*m*/*z* = 5826.1), –TGTA (*m*/*z* = 5513.8), –TGTAAAAC (*m*/*z* = 4282.2) and –TGTAAAACA (*m*/*z* = 3968.8). It is interesting to note that the degradation of strand OD3 by 3′-exonuclease bypassed the first platinated guanine and stopped at the second platinated G on

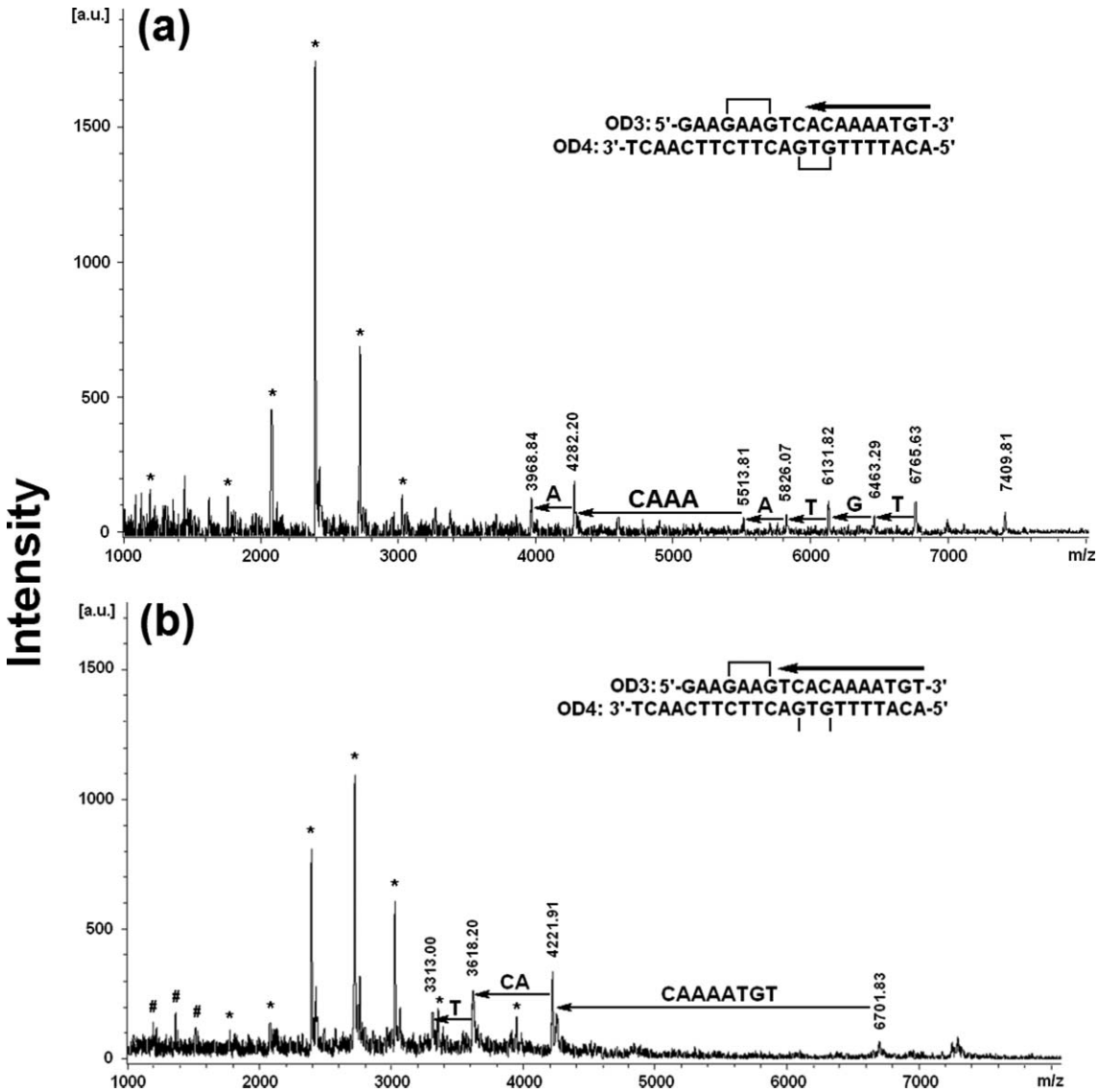

Fig. 7 MALDI-TOF mass spectra of Exo III digests of platinated duplex **N3** by complexes **1** (a) and **2** (b). The arrows indicate the cleavage direction and location along the sequence. Fragments from the unplatinated DNA are indicated by *, and the peaks corresponding to doubly charged ions are marked with #.

the opposite strand. However, exonuclease III digestion of adducts of **2** (Fig. 7b) proceeds with two more nucleotides than that of **1**, resulting in three digestion products by removing the first eleven residues: –TGTAAAAC (m/z = 4221.9), –TGTAAAACAC (m/z = 3618.2) and –TGTAAAACACT (m/z = 3313.0). Detailed assignments for each fragment are given in Table 2.

Exo III is the major repair dsDNA specific nuclease in *Escherichia coli*,[35,37] offering an additional useful tool in determining the cross-links sites[38,39] and the effect of these modifications on DNA tertiary structures.[6] Exo III digestion is inhibited at different sites for DNA adducts of complexes **1** and **2**. The stop site of complex **1** occurs at the second platinated G on the opposite strand, confirming the formation of 1,3-intrastrand cross-links by **1** which disturbs DNA conformation distinctly and consequently hinders further enzymatic digestion. However, in the case of **2**, Exo III proceeds for two more nucleotides and arrests before 1,4-cross-linked guanines, which is consistent with the predominant 1,4-intrastrand cross-links formed by **2**. Therefore, DNA adducts of **1** show more significant inhibitory effects than that of **2** on the DNA digestion by exonuclease III, which is consistent with the

Table 2 DNA fragments after exonuclease III digestion of platinated duplex **N3** by complexes **1** and **2**

Pt complexes	DNA fragments after Exo III digestion	Found	Calcd
1	5′-GAAGAAGTCACAAAATG-3′	6463.3	6461.4
	5′-GAAGAAGTCACAAAAT-3′	6131.8	6132.2
	5′-GAAGAAGTCACAAAA-3′	5826.1	5828.0
	5′-GAAGAAGTCACAAA-3′	5513.8	5514.8
	5′-GAAGAAGTCA-3′	4282.2	4285.0
	5′-GAAGAAGTC-3′	3968.8	3971.8
2	5′-GAAGAAGTCA-3′	4221.9	4222.2
	5′-GAAGAAGT-3′	3618.2	3619.8
	5′-GAAGAAG-3′	3313.0	3315.6

results from CD studies and may explain the higher antitumour efficacy of **1**.

Conclusion

The DNA binding ability and cross-linking patterns of two 1,1/c,c dinuclear platinum(II) complexes **1** and **2**, containing a bridging linker of methylenedianiline or diamino-*p*-xylene respectively, have been investigated and compared. Complex **1**, which binds more strongly to DNA, can readily form equivalent 1,3- and 1,4-intrastrand adducts, whereas **2** predominately gives rise to 1,4- rather than 1,3-intrastrand adducts. The enzymatic digestion of DNA adducts shows that the inhibition site occurs at two nucleotides earlier for complex **1** than for **2**, confirming the distinctive disturbance on DNA conformation induced by cross-links of **1**, which may afford great potential in circumventing resistance pathways that have evolved to eliminate cisplatin.[10,40] These properties may explain why complex **1** exhibits more potent cytotoxicity against A549 cell lines than complex **2** and cisplatin.

Although complexes **1** and **2** share the same {*cis*-$Pt(NH_3)_2$} units, they showed very different DNA binding ability and antitumour property. The linker properties play a determining role in the formation of DNA adducts. The two phenyl rings linked with methylene sp^3-hybridized in **1** allow rapid formation of various DNA adducts and contribute to the high antitumour activity. However, the bridging linker of diamine-*p*-5-xylene in **2** exerts an unfavorable influence on forming cross-links. Therefore, the fine tuning of the nature of linkers, which may vary the Pt $\cdots$ Pt distance and steric hindrance *etc.*, provides a promising strategy in designing 1,1/c,c platinum complexes with the desired DNA binding ability and cross-link patterns.

Acknowledgements

We thank the National Natural Science Foundation of China (No.s 20231010, 20631020, 90713001 and 20721002) and the Natural Science Foundation of Jiangsu Province (BK2008015) for financial support. J. H. Zhu acknowledges funding from the Scientific Research Foundation of Graduate School of Nanjing University.

References

1 N. J. Wheate and J. G. Collins, *Coord. Chem. Rev.*, 2003, **241**, 133–145.
2 J. Reedijk, *Proc. Natl. Acad. Sci. U. S. A.*, 2003, **100**, 3611–3616.
3 A. S. Abu-Surrah and M. Kettunen, *Curr. Med. Chem.*, 2006, **13**, 1337–1357.
4 S. J. Berners-Price, M. S. Davies, J. W. Cox, D. S. Thomas and N. Farrell, *Chem.–Eur. J.*, 2003, **9**, 713–725.
5 A. Hegmans, S. J. Berners-Price, M. S. Davies, D. S. Thomas, A. S. Humphreys and N. Farrell, *J. Am. Chem. Soc.*, 2004, **126**, 2166–2180.
6 J. H. Zhu, Y. M. Zhao, Y. Y. Zhu, Z. Y. Wu, M. X. Lin, W. J. He, Y. Wang, G. J. Chen, L. Dong, J. F. Zhang, Y. Lu and Z. J. Guo, *Chem.–Eur. J.*, 2009, **15**, 5245–5253.
7 J. Kašpárková, J. Zehnulova, N. Farrell and V. Brabec, *J. Biol. Chem.*, 2002, **277**, 48076–48086.
8 J. Y. Zhang, D. S. Thomas, S. J. Berners-Price and N. Farrell, *Chem.–Eur. J.*, 2008, **14**, 6391–6405.
9 M. Kartalou and J. M. Essigmann, *Mutat. Res., Fundam. Mol. Mech. Mutagen.*, 2001, **478**, 1–21.
10 Y. Jung and S. J. Lippard, *Chem. Rev.*, 2007, **107**, 1387–1407.
11 Y. Qu and N. Farrell, *J. Am. Chem. Soc.*, 1991, **113**, 4851–4857.
12 A. J. Kraker, J. D. Hoeschele, W. L. Elliott, H. D. H. Showalter, A. D. Sercel and N. Farrell, *J. Med. Chem.*, 1992, **35**, 4526–4532.
13 J. Kašpárková, O. Nováková, O. Vrána, N. Farrell and V. Brabec, *Biochemistry*, 1999, **38**, 10997–11005.
14 J. W. Cox, S. J. Berners-Price, M. S. Davies, W. Barklage, Y. Qu and N. Farrell, *J. Am. Chem. Soc.*, 2001, **123**, 1316–1326.
15 N. Farrell, in *Advances in DNA Sequence Specific Agents*, ed. J. H. Hurley, J. B. Chaires, JAI Press Inc., Greenwich, CT, 1996, vol. 2, p. 187.
16 J. Kašpárková, J. Zehnulova, N. Farrell and V. Brabec, *J. Biol. Chem.*, 2001, **276**, 22191–22199.
17 M. B. G. Kloster, J. C. Hannis, D. C. Muddiman and N. Farrell, *Biochemistry*, 1999, **38**, 14731–14737.
18 N. Farrell, *in*: L. R. Kelland, N. P. Farrell, (*Eds.*), *Platinum-Based Drugs in Cancer Therapy*, Humana Press, Totowa, 2000, pp. 321.
19 C. Manzotti, G. Pratesi, E. Menta, R. Di Domenico, E. Cavalletti, H. H. Fiebig, L. R. Kelland, N. Farrell, D. Polizzi, R. Supino, G. Pezzoni and F. Zunino, *Clin. Cancer Res.*, 2000, **6**, 2626–2634.
20 N. Farrell, *Met. Ions Biol. Syst.*, 2004, **42**, 251–296.
21 M. E. Oehlsen, Y. Qu and N. Farrell, *Inorg. Chem.*, 2003, **42**, 5498–5506.
22 D. M. Fan, X. L. Yang, X. Y. Wang, S. C. Zhang, J. F. Mao, J. Ding, L. P. Lin and Z. J. Guo, *JBIC, J. Biol. Inorg. Chem.*, 2007, **12**, 655–665.
23 X. Y. Wang and Z. J. Guo, *Dalton Trans.*, 2008, 1521–1532.
24 J. Y. Zhang, X. Y. Wang, C. Tu, J. Lin, J. Ding, L. P. Lin, Z. M. Wang, C. He, C. H. Yan, X. Z. You and Z. J. Guo, *J. Med. Chem.*, 2003, **46**, 3502–3507.
25 W. C. Johnson, *In*: K. Nakanishi, N. Berova, R. W. Woody, (*Eds*), *Circular Dichroism: Principles and Applications*. VCH, New York, 1994, pp. 523–540.
26 M. V. Keck and S. J. Lippard, *J. Am. Chem. Soc.*, 1992, **114**, 3386–3390.
27 W. M. Scovell and F. Collard, *Nucleic Acids Res.*, 1985, **13**, 2881–2895.
28 M. J. Frisch, G. W. Trucks, H. B. Schlegel, G. E. Scuseria, M. A. Robb, J. R. Cheeseman, J. A. Montgomery, Jr., T. Vreven, K. N. Kudin, J. C. Burant, J. M. Millam, S. S. Iyengar, J. Tomasi, V. Barone, B. Mennucci, M. Cossi, G. Scalmani, N. Rega, G. A. Petersson, H. Nakatsuji, M. Hada, M. Ehara, K. Toyota, R. Fukuda, J. Hasegawa, M. Ishida, T. Nakajima, Y. Honda, O. Kitao, H. Nakai, M. Klene, X. Li, J. E. Knox, H. P. Hratchian, J. B. Cross, V. Bakken, C. Adamo, J. Jaramillo, R. Gomperts, R. E. Stratmann, O. Yazyev, A. J. Austin, R. Cammi, C. Pomelli, J. Ochterski, P. Y. Ayala, K. Morokuma, G. A. Voth, P. Salvador, J. J. Dannenberg, V. G. Zakrzewski, S. Dapprich, A. D. Daniels, M. C. Strain, O. Farkas, D. K. Malick, A. D. Rabuck, K. Raghavachari, J. B. Foresman, J. V. Ortiz, Q. Cui, A. G. Baboul, S. Clifford, J. Cioslowski, B. B. Stefanov, G. Liu, A. Liashenko, P. Piskorz, I. Komaromi, R. L. Martin, D. J. Fox, T. Keith, M. A. Al-Laham, C. Y. Peng, A. Nanayakkara, M. Challacombe, P. M. W. Gill, B. G. Johnson, W. Chen, M. W. Wong, C. Gonzalez and J. A. Pople, *GAUSSIAN 03 (Revision D.1)*, Gaussian, Inc., Wallingford, CT, 2004.
29 A. C. G. Hotze, B. M. Kariuki and M. J. Hannon, *Angew. Chem., Int. Ed.*, 2006, **45**, 4839–4842.
30 S. Komeda, S. Bombard, S. Perrier, J. Reedijk and J. Kozelka, *J. Inorg. Biochem.*, 2003, **96**, 357–366.
31 S. Redon, S. Bombard, M. A. Elizondo-Riojas and J. C. Chottard, *Nucleic Acids Res.*, 2003, **31**, 1605–1613.
32 V. Marchán, E. Pedroso and A. Grandas, *Chem.–Eur. J.*, 2004, **10**, 5369–5375.
33 K. S. Schmidt, M. Boudvillain, A. Schwartz, G. A. van der Marel, J. H. van Boom, J. Reedijk and B. Lippert, *Chem.–Eur. J.*, 2002, **8**, 5566–5570.
34 S. D. Merajver, T. M. Pham, R. F. Caduff, M. Chen, E. L. Poy, K. A. Cooney, B. L. Weber, F. S. Collins, C. Johnston and T. S. Frank, *Nat. Genet.*, 1995, **9**, 439–443.
35 S. G. Rogers and B. Weiss, *Methods Enzymol.*, 1980, **65**, 201–211.
36 C. D. Mol, C. F. Kuo, M. M. Thayer, R. P. Cunningham and J. A. Tainer, *Nature*, 1995, **374**, 381–386.
37 W. Linxweiler and W. Horz, *Nucleic Acids Res.*, 1982, **10**, 4845–4859.
38 B. Royer-Pokora, L. K. Gordon and W. A. Haseltine, *Nucleic Acids Res.*, 1981, **9**, 4595–4609.
39 B. Algueró, J. López de la Osa, C. González, E. Pedroso, V. Marchán and A. Granadas, *Angew. Chem., Int. Ed.*, 2006, **45**, 8194–8197.
40 V. Brabec, *Prog. Nucleic Acid Res. Mol. Biol.*, 2002, **71**, 1–68.